





# An experimental approach to the influence of partial rebar corrosion and concrete degradation on behavior of FRP-strengthened RC beams

M. Abbasi<sup>1</sup> · H. Naderpour<sup>1</sup> 

Received: 21 November 2020 / Accepted: 13 August 2021

Published online: 31 August 2021

© The Author(s) 2021 

## Abstract

Human factors are one of the main reasons for structural damage as they decrease the bearing capacity and also lead to an inaccurate estimation of the structure. Previous studies show that the use of CFRP in the damaged structures can significantly increase their bending and shear capacity. This study examines the capacity and cracks distribution in eight RC (reinforced concrete) beams (210 × 250 × 250 cm), each of which was rehabilitated with seven CFRP (carbon fiber-reinforced polymer) strips using the strip method. Each beam, except for the control specimen, experiences different types of concrete and rebar damages, which are finally compared with those of the control specimen. The results indicated that rebar damage in all the beams was significant and the effects of concrete damage were minimized by CFRP strips. Moreover, the force–displacement diagrams indicate the greatest force for the control specimen. Other specimens reached up to 80% of the force experienced by the control specimen. Finally, the parametric study showed that the influence of the crack width on decreasing the bearing capacity was more significant compared with the other parameters.

**Keywords** RC beam · CFRP · Rebar corrosion · Concrete degradation · Composite material

## 1 Introduction

Since the late 1980s, the rehabilitation method using FRP<sup>1</sup> has been implemented by a large number of researchers. In comparison with the other rehabilitation techniques, this method has some advantages, including high strength to weight ratio, high resistance against corrosive materials, flexibility, and ductility [1]. Dong et al. compared the ductility of RC beams rehabilitated with FRP composites with those for the other beams [2]. Choi et al. examined the structural and non-cohesive performance of RC beams reinforced with FRP composites [3].

An alternative reinforcing material, fiber-reinforced polymer (FRP) bar, is being considered as a solution to the corrosion problem. Due to their corrosion resistance, FRP bars have received considerable attention, especially from the

transportation industry. Applications of FRP bars, however, are not only limited to cases where corrosion is of concern. They are also useful in structures requiring magnetic transparency and in members susceptible to chemical attack [4]. Moreover, in another study, the resistance against flexibility was examined and indicated an increase in the shear capacity of RC beams when strengthened by FRP sheets. In the mentioned method, resistance was more effective than the shear ductility. Another study investigated the discontinuity of FRP on all surfaces because of the cracks and their spread in the damage state [5].

When a structural element is vulnerable to such effects, the fastest and most cost-effective way to prevent damage is to strengthen the element. In the past, the typical methods of shear strengthening of vulnerable RC members involved adding extra RC or steel elements. The

<sup>1</sup> Fiber-reinforced polymer.

✉ H. Naderpour, naderpour@semnan.ac.ir | <sup>1</sup>Faculty of Civil Engineering, Semnan University, Semnan 3513119111, Iran.



traditional methods most commonly used to increase the shear capacity of RC members are (a) adding reinforcement around the cross section and placing concrete around it (concrete jacket) [6].

From the environmental and economic viewpoints, repairing, reviving, and rehabilitating the existing structures are preferred to their demolishing and rebuilding. Furthermore, rehabilitation projects are implemented faster than new projects. Moreover, the new projects put such structures out of operation [7–9] examined the effect of parameters such as the preparation of a concrete surface, cohesive material, and concrete strength on adherence strength and found out that preparing the concrete surface would increase the adherence strength by 3–11% [10].

Many different fractures of RC beams reinforced with FRP sheets have been observed in experimental studies. These fractures are highly diverse, as some researchers have reported more than 30 different fracture cases. According to the previous studies, different kinds of bending damage in rehabilitated specimens are (1) yielding of longitudinal bars along with the fracture of fiber polymers; (2) concrete crushing under compression before the fracture of fiber polymers; (3) separation of the polymer fiber ends from the concrete surface along with the concrete cover of longitudinal rebars; (4) separation of the polymer fiber ends from the concrete surface, and a part of the concrete cover (a rare case); (5) separation of the polymer fiber ends from the concrete surface and a part of the concrete cover because of bending cracks; and (6) separation of polymer fiber ends from the concrete surface and a part of the concrete cover because of bending-shear cracks. According to the experimental studies, the cases 4–6 are more observed in beams without transverse reinforcements [11].

In this regard, Kotynia and Cholostiakow exploited the advantages of these two methods and tested nine full-scale beam specimens [12]. They presented a new method, which resulted in higher stiffness and bearing capacity and significantly decreased the beam deflection in the middle of the span. Almusallam et al. examined 11 bending beams (225 × 200 × 150 mm) and analyzed them using the FEM.<sup>2</sup> They concluded that increasing the tension rebar percentage in non-reinforced beams decreases the ductility of the deflections, as well as the effects of FRP sheets on increasing bending capacity [13].

The type of rehabilitation with FRP to repair the concrete structures depends on the geometrical and mechanical properties of the system. U-type reinforcements, longitudinal elements, FRP straps, and FRP strips are some conventional rehabilitation methods using FRP which have been utilized experimentally and numerically by previous researchers [6, 14–23].

While a structural element is subjected to detrimental factors, the fastest and the most expensive method to stop the damage spread is rehabilitating the structure. In the past, rehabilitation was mostly limited to adding RC or steel elements [24]. The life span of concrete structural elements highly depends on their repair and rehabilitation. Due to the mistakes and recommendations of bylaws, the structures encounter many dangers. Unacceptable physical and chemical conditions or construction errors make the practitioners use the rehabilitation covers to reinforce the fractured ductile elements [25]. The major contribution to FRP composites is its potential to extend service life of existing structures [26]. The failure mode of completely wrapped beams is FRP rupture, which is more favorable compared to the sudden debonding of the FRP laminates of the U-Wrapped beams. In the case where beams cannot be completely wrapped, the U-wrapping scheme is a feasible option. However, for the U-Wrapped beams to reach the same performance of the completely wrapped beams, CFRP laminates should be properly anchored to avoid the brittle debonding [27, 28].

The main objective of this study is to truly evaluate the behavior of RC beams having rebar or concrete damage and rehabilitated with CFRP composites. With using concrete beams and bonding CFRP sheets together in strips, the ultimate bending resistance and displacement in the beam were determined. For this purpose, eight RC beams (2100 × 250 × 250 mm) strengthened with CFRP strips were manufactured. Each beam had a specific pre-damage in the rebar and/or concrete. These specimens were subjected to four-point bending, and the results were compared with those of the control specimen in order to evaluate the efficiency of the rehabilitation technique.

## 2 Test layout

### 2.1 Test specimens

In this study, eight full-scale RC beams were manufactured and tested. All the specimens had 2100 mm length and a square surface (250 mm × 250 mm). Since the study purpose was to examine the fracture of the beams with internal damage and to detect the crack spread pattern, the specimens were allowed (based on ACI 318) to experience bending cracks. Moreover, a control specimen, with no concrete or rebar damage, was utilized to compare the results of the rehabilitated beams. The amount of the used rebar was 1.23%. The size of steel reinforcements was  $\phi 10@200$  mm. In accordance with the rebar layout, the span to effective depth ratio ( $a/d$ ) of the beams was equal to 2.65. The specimens were procured and then tested by a hydraulic jack using a four-point loading. The

<sup>2</sup> Finite element method.

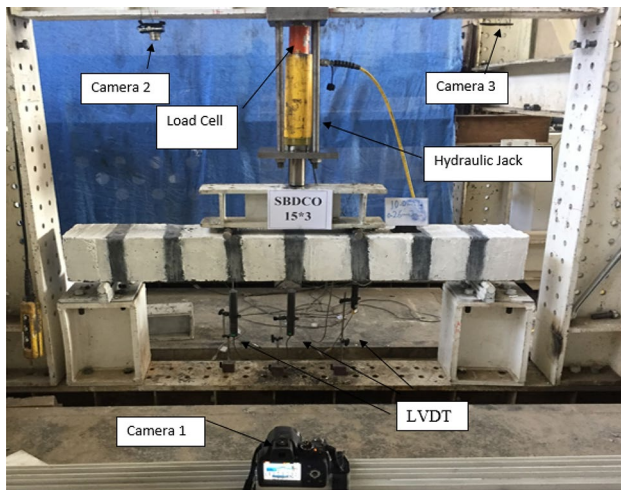


**Fig. 1** Details of the test setup and location of cameras and LVDTs

area between the two-point loads had a constant moment and zero shear. In this area, the beam behavior under pure bending could be evaluated. In the area between each load point and the closest support, the combined effect of bending and shear loads can be examined. Static and uniform loads were applied. According to Fig. 1, the middle-point displacement and force can be transferred to the data logger device by LVDT<sup>3</sup> and the load cell, respectively. Further, the experimental displacement in the middle of RC beams reinforced with FRP was determined. Using the load–displacement diagrams from the tests, the beam displacements were determined in different load levels and bearing capacities of the beams reinforced with FRP. Moreover, the observations were recorded in each stage, and the crack spread pattern was illustrated to determine the beam failure mechanism.

The manufactured beams were divided into two categories based on their damage type: beams with concrete damage and beams with rebar damage. Rebar damage includes two 25 mm corruptions and a decrease in the rebar diameter by half (7 mm) of the length of the bottom rebars. The beams were reinforced with FRP strips. According to the beam perimeter (100 mm), some extra strip lengths were considered for the overlaps (150 mm) in order to maintain the necessary connection and strength. The FRP width is 80 mm, and it is located 200 mm on either side of the middle point. In the case of concrete damage, special foams with different widths and depths were utilized in order to simulate the damage. All the posed damages are shown in Table 1.

The beams were reinforced with FRP strips. According to the beam perimeter (100 mm), some extra strip lengths

were considered for the overlaps (150 mm) in order to maintain the necessary connection and strength. The FRP width is 80 mm, and it is located 200 mm on either side of the middle point. According to Fig. 2, seven FRP strips are installed on each beam. One failure in BDRA samples and two failures in BDRS samples were located in one-third of the effective span of the fixed-end beam with a distance of 60 cm from the two head supports. It is machined accurately and evenly using a turning tool such that to cause failure. The reinforcement's diameter is reduced from 14 to 7 mm (Fig. 3).

## 2.2 Material properties

According to the compressive strength tests conducted on the cubic specimens of the concrete used for the beams (with 150 mm dimension), the average compressive strength was 35 MPa. In this study, maximum gravel size and the specific gravity were 12 mm and 2.6 g/cm<sup>3</sup>, respectively. Moreover, the water absorption rate of the specimen was 1%. The gravel grading curve was based on ASTM C33. The sand size was a combination of 0–3 mm and 3–6 mm. Its specific gravity was 2.65 g/cm<sup>3</sup>, and the water absorption rate was 1.45%. The sand grading curve was based on ASTM C33. Cement type II with a specific gravity of 3.15 g/cm<sup>3</sup> was used.

In order to reinforce the concrete and manufacture the RC beams, 10-mm and 14-mm rebars were used. The 10-mm rebars were used for internal reinforcements, and 14-mm rebars were utilized for longitudinal reinforcements. The rebar layout is shown in Fig. 2. Rebar yielding strength was measured according to ISO 6982-1 as such three specimens with 75-cm length were selected and used for uniaxial tension test.

The average yielding strength for 10- and 14-mm rebars was 417 and 435 MPa, respectively. FRP strips, QUANTOM Wrap 200C, and epoxy resins, QUANTUM EPR 3001, were used for rehabilitation. According to the properties noted in the manufacturer's catalog, the tensile strength for this composite material is 4950 MPa. Tensile E-modulus is 240 GPa, and the elongation ratio is 1.5%. Density is 1.8 g/cm<sup>3</sup>, areal weight is 200 g/m<sup>2</sup>, and the thickness is 0.111 mm.

## 2.3 Rehabilitation steps

The eight specimens were manufactured and rehabilitated with FRP strips with 10-mm overlaps. Rehabilitation with FRP was performed based on the following steps (Fig. 3):

1. First, a brush was used to smoothen the concrete surface of the beam. Then, the beam was washed to remove the dust and prepare it for FRP installation [29].

<sup>3</sup> Linear variable displacement transducer.

**Table 1** Details of beam specimens

No.	Specimen	Specimen Details	Description	Purpose of manufacturing
1	SCB (Strengthened Control Beam)		Control reinforced concrete beam	Comparing with other specimens
2	SBDRS (Strengthened Beam Damaged Rebars Symmetric)		Reinforced concrete beam with symmetric rebar corrosion	Comparing with SBDR specimen
3	SBDR (Strengthened Beam Damaged Rebars Asymmetric)		Reinforced concrete beam with one-sided rebar corrosion	Comparing with SBDR specimen
4	SBDCM15*3 (Strengthened Beam Damaged Concrete Mid 15*3)		Reinforced concrete beam with rebar corrosion in the middle (3*15 cm)	Comparing with SBDCO15*3 specimen
5	SBDCO15*3 (Strengthened Beam Damaged Concrete One-third 15*3)		Reinforced concrete beam with rebar corrosion in 1/3 length (3*15 cm)	Comparing with SBDCM15*3 specimen
6	SBDCM10*3 (Strengthened Beam Damaged Concrete Mid 10*3)		Reinforced concrete beam with rebar corrosion in the middle (3*10 cm)	Comparing with SBDCM15*3 specimen
7	SBDCM15*1 (Strengthened Beam Damaged Concrete Mid-15*1)		Reinforced concrete beam with rebar corrosion in the middle (1*15 cm)	Comparing with SBDCM15*3 specimen
8	SBDCM15*1+10*.5 (Strengthened Beam Damaged Concrete M15*1+O10*.5)		Reinforced concrete beam with rebar corrosion in middle (1*15 cm) and 1/3 length (0.5*10)	Comparing with SBDCM15*3 And SBDCM10*3 specimen



**Fig. 2** Corrosion method of rebar



**Fig. 3** Longitudinal and transverse rebars and their layout

2. FRP strips with 8-mm width and 110-mm length were provided.
3. A combination of adhesive and resin, with a ratio of 1 to 3, was prepared. This proportion would result in maximum strength.
4. Seven FRP stripes were installed on the RC beam, 72 h before testing the specimens.

## 2.4 Test procedure

Figure 4 shows the details of the loading on the beams. In RC beams, compressive jacks applied the force in 60-cm spaces using a plate. The space between the support and

the beam edge was 15 cm, and the 4-point loading was used for testing. In each test, three LVDTs were used to measure the beam deflection in the damage process. One LVDT was placed in the middle point, and the other two were placed in a 20-cm space at either side of the middle span.

Electric strain gauges were installed on each beam to control the response of bending rebars (Fig. 4). Loading was done using a hydraulic jack with 1000-kN capacity.

It is placed in the middle of the beam opening to measure the vertical displacement of the specimens and also at two points of one-third of the LVDT opening. It is connected to the data logger via telephone wire, and all



**Fig. 4** FRP strips preparation

**Table 2** Test results for RC beam specimens

Specimen	Load corresponding to the first crack (kN)	Maximum deflection in the middle point of the beam (mm)	Test ultimate load (kN)	The ratio of test ultimate SBC load to ultimate load of the specimen
SBC	26	75	188	1
SBDCM (10-0.5)(15-1)	41	61	159	0.85
SBDCM (10-3)	26	82	159	0.85
SBDCM (15-1)	29	75	171	0.91
SBDCM (15-3)	40	71	152	0.81
SBDCO (15-3)	38	80	174	0.93
SBDR A	17	70	52	0.28
SBDR S	27	80	50	0.26

information is stored in it every second in all experiments. The LVDT used shows a maximum rise of 20 cm. The load cell is used to create a compressive force and is applied by the plate as a four-point force. Its capacity is 50 tons, which is gradually applied to the desired point.

### 3 Test results

Before applying any loading to the beam, a large number of micro-cracks appeared in the concrete, in the space between coarse aggregates and mortar. Accordingly, the spread of these cracks during loading leads to a nonlinear response of concrete under low stress and an increase in concrete volume close to the damage point. These micro-cracks might be the result of segregation, bleeding, or thermal expansion in mortar during the loading process. This is caused by the difference between the stiffness in aggregates and mortars. The concrete tensile strength is much lower than its compressive strength, and the tension area is prone to cracking when it reaches the tensile strength. In RC beams, the cracks are inevitable if the load

increases; hence, in the preliminary stages of loading, crack or cracks appear on critical points, where the maximum bending moment is present. With an increase in load size, other areas reaching the concrete tensile strength start to crack. Table 2 shows the results for the load of the first cracking, bearing capacity, and the middle-point deflection in the maximum loading according to test results. It can be noticed that the rebar damage has the greatest impact on the strength of RC beams. In the beam SBDRS, with rebar damage in two sides, the bearing capacity, in comparison with the control specimen, decreased by 74%.

The following diagram shows the force–displacement of the control beam, specimens with damage in the middle point, and specimens with different concrete damages. According to Fig. 5, the beam with two damages has the least deflection and bearing capacity among all the beam specimens. When comparing the beams with damage in the same location, it was revealed that the beam with less damage width has the highest bearing capacity.

In Fig. 6, the control concrete beam is compared with specimens having two types of rebar damage. It can be noticed that the exerted force and absorbed energy are

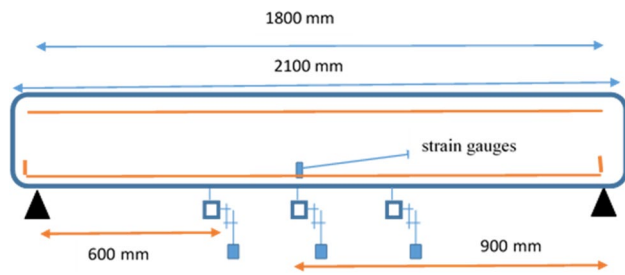


**Fig. 5** Schematic view of the beam layout, loading and measurement instruments

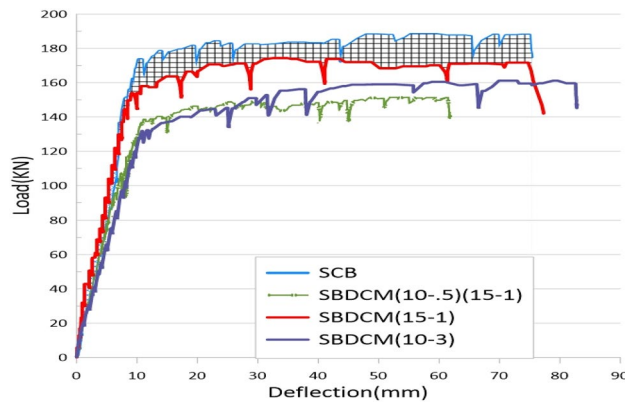


**Fig. 6** Load-displacement diagrams of specimens having degradation in the middle

significantly different in these specimens. The specimen with symmetric rebar damage has lower energy absorption, and its bearing capacity is decreased by 7%. As can be seen, despite the weakness and crack in the concrete, the load-carrying capacity of the control and damaged beams is similar due to the use of CFRP. In another research, the use of reinforcement has increased the load-carrying capacity and compensated for the defect in concrete.

The main reason for using this method for reinforcement and the intentional creation of damage in the rebar and the concrete is that concrete cracks and rebar corrosion are very common in the construction industry. Furthermore, this concrete reinforcement method is simple, practical, and readily available. Accordingly, we have employed this method for reinforcement analysis in order to prevent load-carrying weakness in beams [30].

In Fig. 7, the control specimen is compared with the two other specimens having similar damages. In one specimen, damage is located in the middle, and damage in the other ones is located in the 1/3 point of the beam span. It can be mentioned that the latter endured more force and displacement and has more energy absorption rate. The control specimen has identical reinforcement and

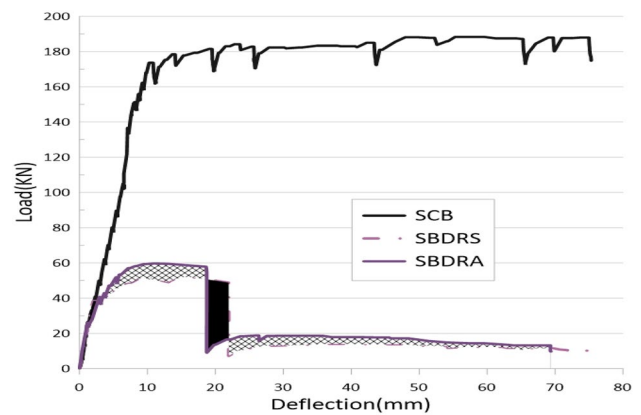


**Fig. 7** Load-displacement diagrams of specimens having corroded rebars

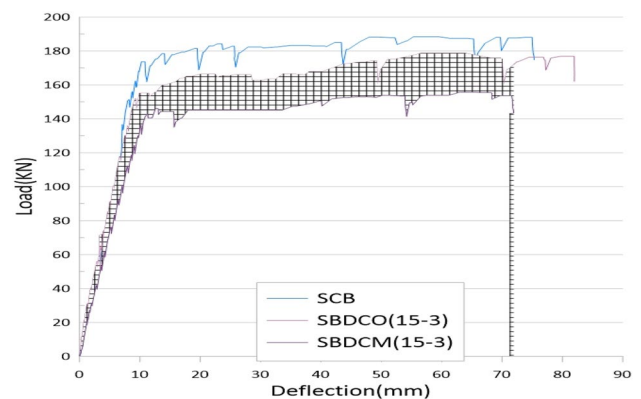


**Fig. 8** Load-displacement diagrams in specimens having the same damage

thus similar displacement. Its bearing capacity, however, increased 14% and compared with the specimen with middle span damage.

In Fig. 8, the control beam is compared with the specimens with central damage and with different widths and heights. It can be observed that the damage width is much more effective than the other variables. The specimens with greater damage width and lower height show more displacement under the less force.

In Fig. 9, the blank sample was compared with center-damaged samples with different widths and heights. As shown in the figure, the effect of damage is higher in the width than in the height. However, samples containing damage with larger width and smaller height exhibit smaller displacement for a smaller force.

According to Fig. 10, damage in the rebar has a great impact on reducing the bearing capacity. Also, this sample has less bearing capacity compared to other samples that have damage in concrete. The SCB sample has the highest

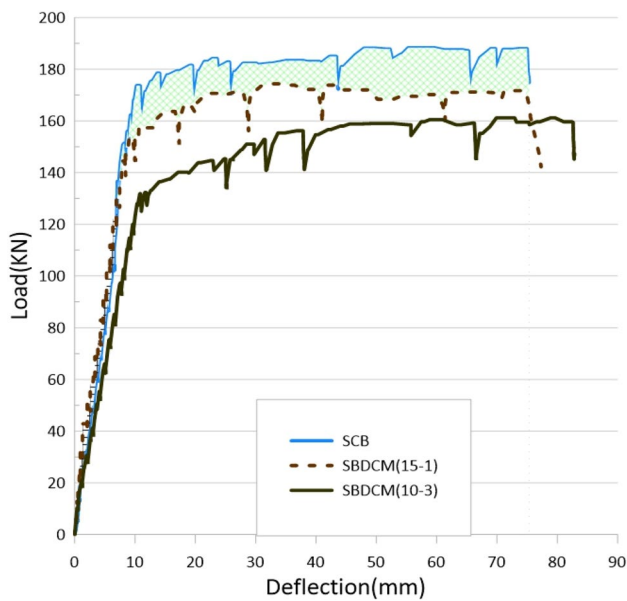


**Fig. 9** Load–deflection of specimens with different damage widths and heights

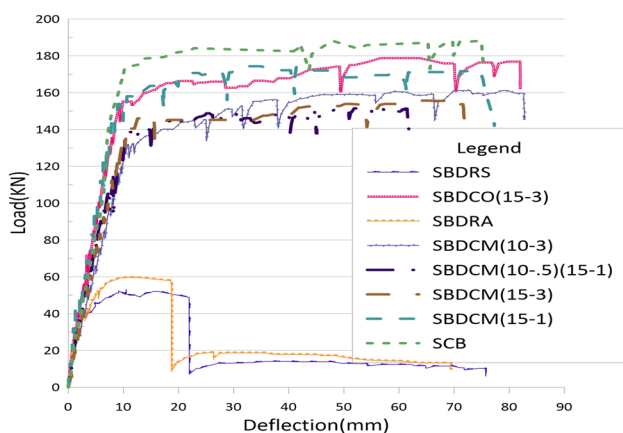


**Fig. 10** Comparison of load–displacement for all specimens

load capacity and then damage in one-third of the opening as expected. However, despite the use of CFRP, the bearing capacity of all samples is very close to each other and this can be considered as a very important point in strengthening the beams. Notably, the bearing capacity of all samples is very close to each other despite the use of CFRP. This can be considered a very important point in strengthening the beams.

#### 4 State of failure

Figure 11 shows the post-failure states for RC beams. As can be seen, the specimens have bending cracks, and the cracks are centered at the vertical direction. These cracks

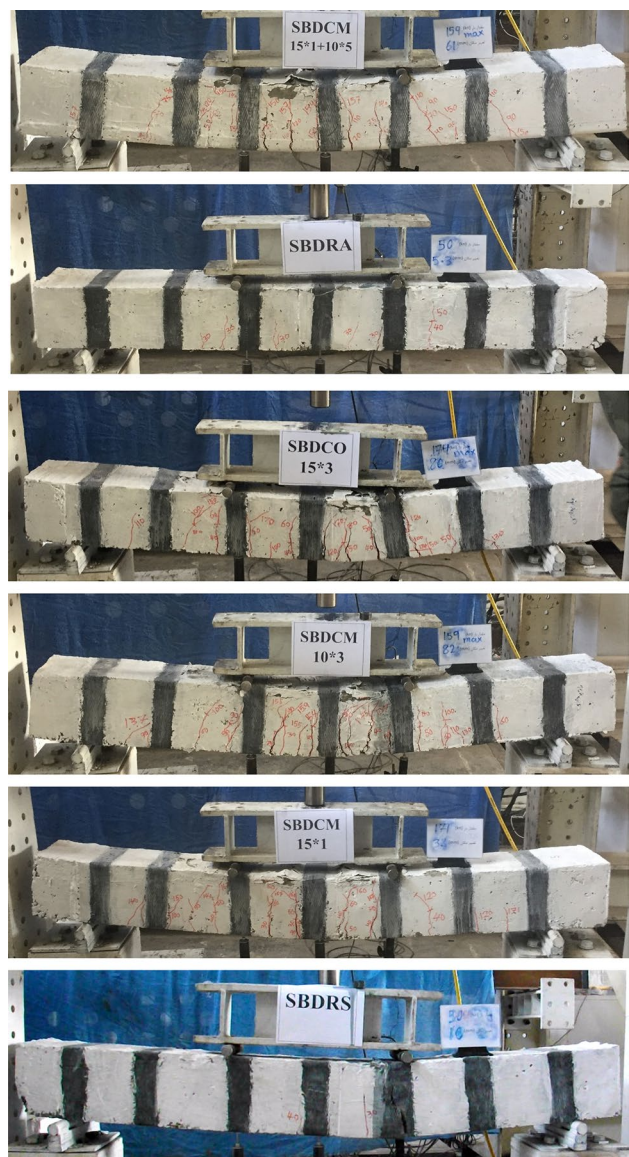


**Fig. 11** Crack spread pattern of specimens corresponding to the fracture moment

start from the bottom of the beam and spread upward. In the control specimen, the cracks are fully distributed. Getting away from the beam center would result in an increase in the crack angles. If the load increases, cracks will develop. Eventually, when the transverse rebars yield, the beam will reach its maximum loading capacity. In SBDCM 15\*1 specimen, since the damage is located in the middle, the cracks are vertical and placed in the middle. With getting away from the middle point, cracks incline, and the crack concentration is in the vicinity of the damage region (Fig. 11) [31]. In the specimens with rebar damage, specimen fractures from the rebar damage region occur quickly. Moreover, in the SBDRS specimen, since FRP is used in the rebar damage region, composite fractures occurred (Fig. 12).





Fig. 12 Rebar failure pattern in SBDRS

Numerous studies have been conducted on the behavior of reinforced concrete Strengthened with FRP. In most cases, due to the outer connection of the reinforcement (FRP), the system always suffers from fracture. Numerous solutions have been proposed to resolve this issue. Here, no fracture of the FRP strips was witnessed since correct connection and coating were observed [32].

In other specimens with some sort of damage, concrete and rebar reached their maximum bearing capacity, and the beam reached the ultimate damage.

## 5 Strains in longitudinal rebars

Figure 11 shows the strains observed in the longitudinal rebars, which are measured by strain gauges installed on the point where the load was applied. The diagrams represent that in the initial phase of loading, the strain is minimal, and the curves are almost similar. However, with an increase in loading, each curve shows its specific trend, and different longitudinal rebars experience different strains. These curves demonstrate that shear reinforcement affects the strains in the longitudinal rebars.

As shown in Figs. 13 and 14, under similar loading conditions, the specimen with greater heights experience more strain in comparison with the other similar specimens. The comparison of the specimens with the control specimen indicated that the control beam demonstrates fewer rebar strains since the concrete can help the rebar in this regard.

In Fig. 15, the damaged specimens are compared with the control specimen. As presented, the damaged beam experiences less strain under similar loading conditions. It might be attributed to the role of the rebar. In addition to the existing failures, the main load is also applied to the rebar; therefore, it reaches the control specimen strain at a higher load level. The diagram path does not change much, and there is no obvious difference with the samples containing concrete damage. The reason is that comparing

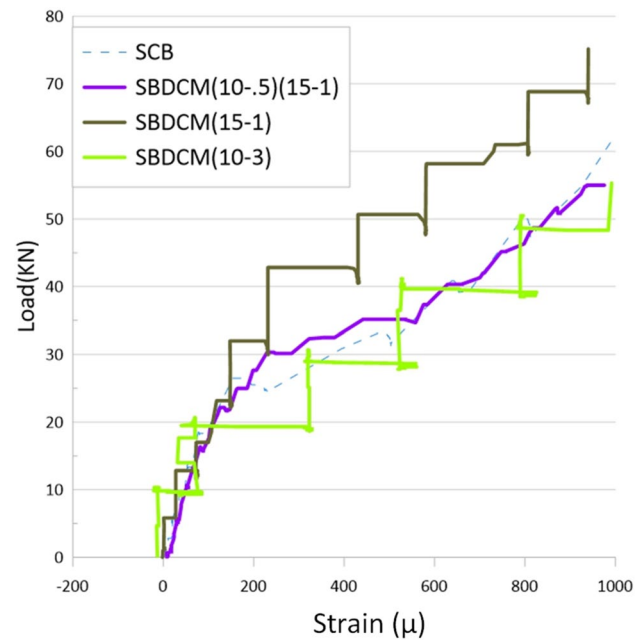


Fig. 13 Load–strain curves for three specimens compared to those of the control beam

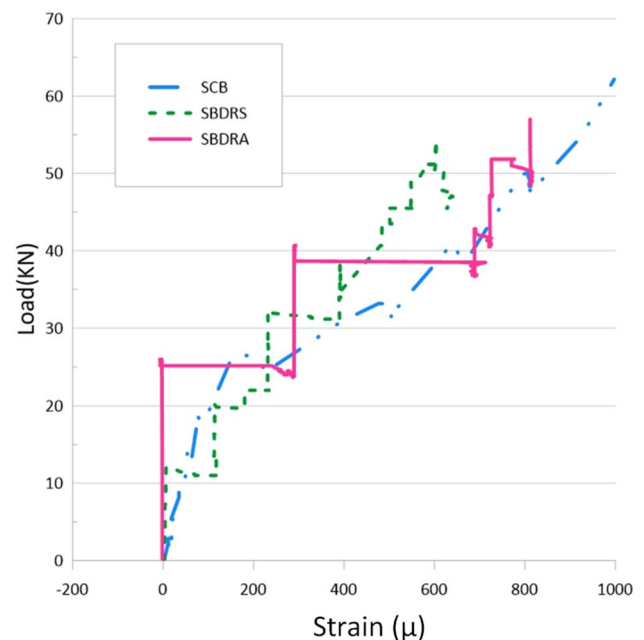
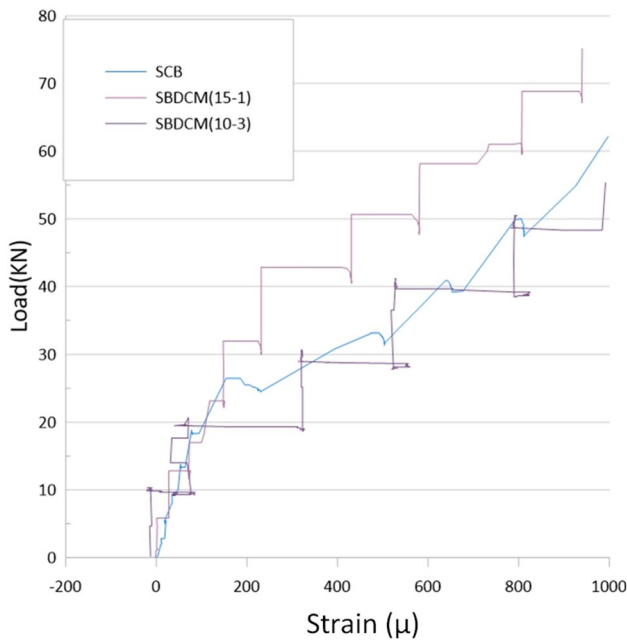
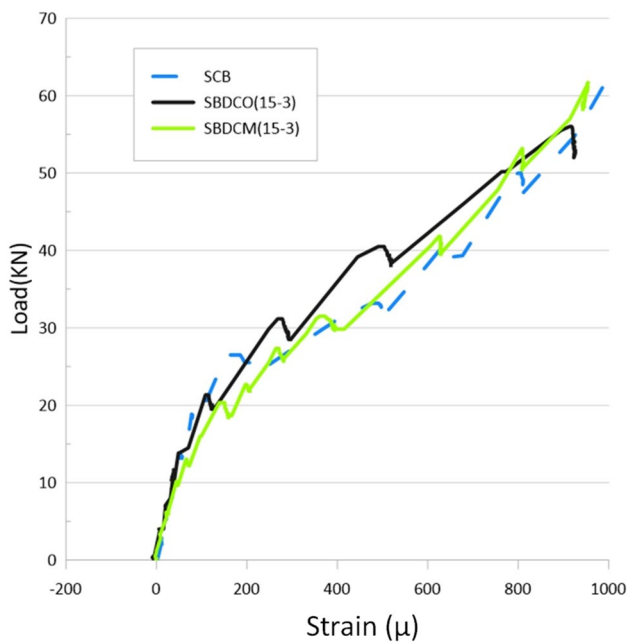


Fig. 14 Load–strain curves for two specimens compared to those of the control beam

the damaged samples with the control sample shows the same shear reinforcement is used in all samples (Figs. 13, 14, 15, 16). In particular, Fig. 16 shows that the SBDCM (15-3) & SBDCO (15-3) samples overlap with the SCB sample.



**Fig. 15** Load–strain curves for two specimens compared to those of the control beam



**Fig. 16** Load–strain curves for two specimens compared to those of the control beam

## 6 Energy

The area under the force–displacement curve is the energy absorbed by the structure. This energy can be

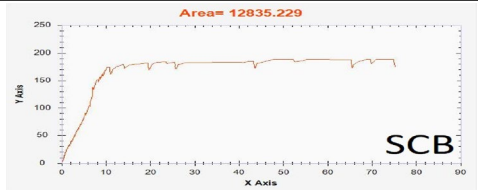
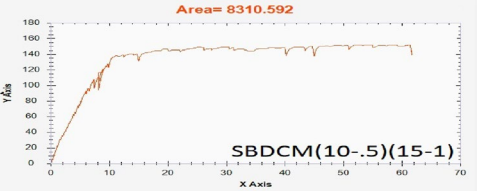
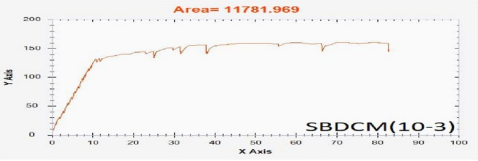
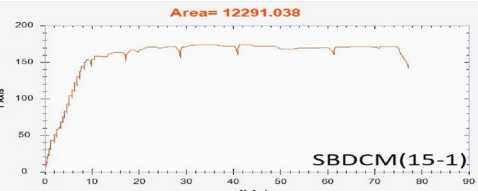
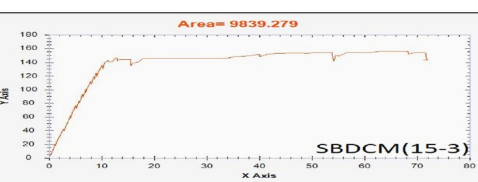
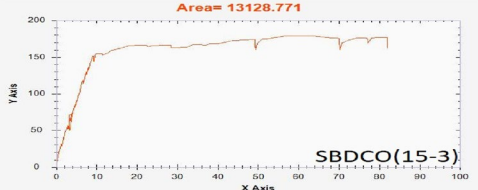
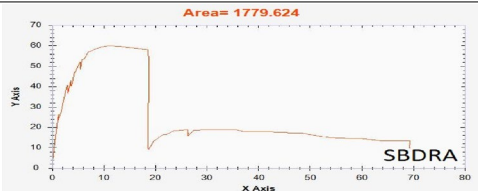
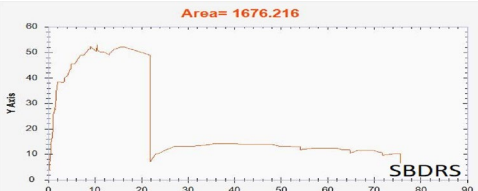
examined during earthquakes and higher structure performances. Table 3 shows the area under the force–displacement curve for eight manufactured beams. The smallest and largest values are for SBDRS and SBDCO specimens, respectively (15-3). The two concrete beams with rebar damage, in comparison with the control beam, only managed to absorb as much as 13% of the existing energy. For SBDCM (10-3) and SBDCM (15-1) specimens, the values were more than 90%.

## 7 Conclusion

In this study, eight full-scale RC beams were manufactured and tested in order to reveal the response of the beams reinforced with FRP sheets. The effects of parameters such as rebar damages (decreasing diameter in the middle section and the 1/3 of the total length) and concrete damages (cracks with different widths and heights located in the middle or 1/3 of the total length) were examined. The following conclusions were made:

- In all the manufactured specimens, bending failure occurs, and cracks are vertical in the middle and inclined in the sides. According to the location of the concrete failure in the beam, the crack concentration is higher in the concerned areas. In specimens with rebar damages, the beam is not extensively cracked, and cracking is limited to the location of the damage.
- Bearing capacity of the control beam with no particular damage is greater than all the other specimens'. The least bearing capacity is for the specimens with rebar damages. The least beam deflection is for the specimens with two damages. The most deflection is for specimens with rebar damages. This might be related to the specimen fracture.
- In all the specimens, a fracture occurs out of the FRP reinforcement region. It demonstrates the stability of the reinforced section. However, the FRP sheet located in the middle was fractured during the final loading.
- In all the beams, except the second beam with rebar damages, high ductility, and energy absorption rates were observed. Although these rates are lower compared to that of the control specimen, they could be completely acceptable and approved with respect to the damages. It can be concluded that the use of FRP and limited damage in concrete would result in a slight decrease in the bearing capacity, even though the energy absorption rate is satisfactory.
- The strains in the longitudinal rebars, located under the loading area, demonstrate that greater strain is

**Table 3** The area under the curve for concrete specimens

Name	The area under the curve	NO/SCB	Diagram shape	Rank (among 8 beam specimens)
SBC	12,835.229	1		2
SBDCM (10-0.5)(15-1)	8310.592	0.647		6
SBDCM (10-3)	11,781.969	0.918		4
SBDCM (15-1)	12,291.038	0.958		3
SBDCM (15-3)	9839.279	0.767		5
SBDCO (15-3)	13,128.771	1.023		1
SBDR	1779.624	0.139		7
SBDRS	1676.216	0.131		8

observed under the same loading conditions in concrete damages with larger widths. In addition, specimens with rebar damages sustain much less strain under the same loading conditions.

**Funding** This research received no external funding.

**Data availability** The raw/processed data required to reproduce these findings cannot be shared at this time as the data also form part of an ongoing study.

## Declarations

**Conflict of interest** The authors declare no conflict of interest.

**Ethical approval** This article does not contain any studies with human participants performed by any of the authors.

**Open Access** This article is licensed under a Creative Commons Attribution 4.0 International License, which permits use, sharing, adaptation, distribution and reproduction in any medium or format, as long as you give appropriate credit to the original author(s) and the source, provide a link to the Creative Commons licence, and indicate if changes were made. The images or other third party material in this article are included in the article's Creative Commons licence, unless indicated otherwise in a credit line to the material. If material is not included in the article's Creative Commons licence and your intended use is not permitted by statutory regulation or exceeds the permitted use, you will need to obtain permission directly from the copyright holder. To view a copy of this licence, visit <http://creativecommons.org/licenses/by/4.0/>.

## References

- Erki MA, Meier U (1999) Impact loading of concrete beams externally strengthened with CFRP laminates. *J Compos Constr* 3(3):117–124
- Dong J, Wang Q, Guan Z (2013) Structural behaviour of RC beams with external flexural and flexural–shear strengthening by FRP sheets. *Compos Part B Eng* 44(1):604–612
- Choi E, Utui N, Kim HS (2013) Experimental and analytical investigations on debonding of hybrid FRPs for flexural strengthening of RC beams. *Compos Part B Eng* 45(1):248–256
- Tureyen AK, Frosch RJ (2002) Shear tests of FRP-reinforced concrete beams without stirrups. *Struct J* 99(4):427–434
- Bonacci JF, Maalej M (2001) Behavioral trends of RC beams strengthened with externally bonded FRP. *J Compos Constr* 5(2):102–113
- Täljsten B (2003) Strengthening concrete beams for shear with CFRP sheets. *Constr Build Mater* 17(1):15–26
- Yao J, Teng JG, Lam L (2005) Experimental study on intermediate crack debonding in FRP-strengthened RC flexural members. *Adv Struct Eng* 8(4):365–396
- Teng JG, Smith S-T, Yao J, Chen J-F (2003) Intermediate crack-induced debonding in RC beams and slabs. *Constr Build Mater* 17(6–7):447–462
- Klamer EL, Hordijk DA, Hermes MCJ (2008) The influence of temperature on RC beams strengthened with externally bonded CFRP reinforcement. *Heron* 53(3):157–185
- Chajes MJ, Finch WW, Thomson TA (1996) Bond and force transfer of composite-material plates bonded to concrete. *Struct J* 93(2):209–217
- Oehlers DJ (2001) Development of design rules for retrofitting by adhesive bonding or bolting either FRP or steel plates to RC beams or slabs in bridges and buildings. *Compos Part A Appl Sci Manuf* 32(9):1345–1355
- Kotynia R, Cholostiakow S (2015) New proposal for flexural strengthening of reinforced concrete beams using CFRP T-shaped profiles. *Polymers (Basel)* 7(11):2461–2477
- Almusallam TH, Elsanadedy HM, Al-Salloum YA (2015) Effect of longitudinal steel ratio on behavior of RC beams strengthened with FRP composites: experimental and FE study. *J Compos Constr* 19(1):4014028
- Jumaat MZ, Alam MA (2008) Behaviour of U and L shaped end anchored steel plate strengthened reinforced concrete beams. *Eur J Sci Res* 22(2):184–196
- Haddad RH, Marji CS (2019) Composite strips with U-shaped CFRP wrap anchor systems for strengthening reinforced concrete beams. *Int J Civ Eng* 17(11):1799–1811
- Yoshitake I, Yumikura K, Mimura Y, Kim Y-J (2011) Composite strips with various anchor systems for retrofitting concrete beams. *Int J Concr Struct Mater* 5(1):43–48
- Shahriari S, Naderpour H (2020) Reliability assessment of shear-deficient reinforced concrete beams externally bonded by FRP sheets having different configurations. *Structures* 25:730–742
- Naderpour H, Alavi SA (2017) A proposed model to estimate shear contribution of FRP in strengthened RC beams in terms of adaptive neuro-fuzzy inference system. *Compos Struct* 170:215–227
- Ahmed E, Sobuz HR, Sutan NM (2011) Flexural performance of CFRP strengthened RC beams with different degrees of strengthening schemes. *Int J Phys Sci* 6(9):2229–2238
- Moradi E, Naderpour H, Kheyroddin A (2020) An experimental approach for shear strengthening of RC beams using a proposed technique by embedded through-section FRP sheets. *Compos Struct* 238:111988
- Nguyen-Xuan H, Thai CH, Nguyen-Thoi T (2013) Isogeometric finite element analysis of composite sandwich plates using a higher order shear deformation theory. *Compos Part B Eng* 55:558–574
- Wu Y-F, Huang Y (2008) Hybrid bonding of FRP to reinforced concrete structures. *J Compos Constr* 12(3):266–273
- Haji M, Naderpour H, Kheyroddin A (2019) Experimental study on influence of proposed FRP-strengthening techniques on RC circular short columns considering different types of damage index. *Compos Struct* 209:112–128
- A. C. I. Committee and I. O. for Standardization (2008) Building code requirements for structural concrete (ACI 318–08) and commentary. A. C. I. Committee and I. O. for Standardization, Indianapolis
- Haddad RH, Shannag MJ, Hamad RJ (2007) Repair of heat-damaged reinforced concrete T-beams using FRC jackets. *Mag Concr Res* 59(3):223–231
- Haddad RH, Shannag MJ, Moh'd A (2008) Repair of heat-damaged RC shallow beams using advanced composites. *Mater Struct* 41(2):287–299
- Mhanna HH, Hawileh RA, Abdalla JA (2019) Shear strengthening of reinforced concrete beams using CFRP wraps. *Procedia Struct Integr* 17:214–221. <https://doi.org/10.1016/j.prostr.2019.08.029>
- Naser MZ, Hawileh RA, Abdalla JA (2019) Fiber-reinforced polymer composites in strengthening reinforced concrete

- structures: a critical review. *Eng Struct* 198(November):109542. <https://doi.org/10.1016/j.engstruct.2019.109542>
29. Chen C et al (2019) Mechanism of surface preparation on FRP-Concrete bond performance: a quantitative study. *Compos Part B Eng* 163:193–206
  30. Leung CKY, Chen Z, Lee S, Ng M, Xu M, Tang J (2007) Effect of size on the failure of geometrically similar concrete beams strengthened in shear with FRP strips. *J Compos Constr* 11(5):487–496
  31. Zhou A, Qin R, Feo L, Penna R, Lau D (2017) Investigation on interfacial defect criticality of FRP-bonded concrete beams. *Compos Part B Eng* 113:80–90
  32. Chen J-F, Teng J-G (2003) Shear capacity of FRP-strengthened RC beams: FRP debonding. *Constr Build Mater* 17(1):27–41

**Publisher's Note** Springer Nature remains neutral with regard to jurisdictional claims in published maps and institutional affiliations.